

Nonlinear ac susceptibility studies of high- T_c rings: Influence of the structuring method and determination of the flux creep exponent

S. Streubel, F. Mrowka, M. Wurlitzer, and P. Esquinazi

Abteilung Supraleitung und Magnetismus, Institut für Experimentelle Physik II, Universität Leipzig, Linnéstrasse 5, D-04103 Leipzig, Germany

K. Zimmer

Institut für Oberflächenmodifizierung e.V., D-04138 Leipzig, Germany

We have studied the influence of the patterning procedure on the critical current density of high- T_c $\text{YBa}_2\text{Cu}_3\text{O}_{7-\delta}$ thin rings using the nonlinear ac susceptibility method. At no applied dc magnetic field we have found that laser ablation degrades strongly the critical current density whereas ion beam etching has only a weak influence on it. From the measurements at different frequencies and dc magnetic fields we analyzed the influence of flux creep and obtained the field dependence of the flux creep exponent. Our data reconfirm the recently observed scaling relation for the nonlinear susceptibility response of type-II superconductors.

74.72.Bk, 74.76.Bz, 74.60.Jg

I. INTRODUCTION

In a recently published letter we have shown that the measurement of the magnetic moment of samples with ring geometry enables the identification of regions with degraded superconducting regions and can be used as a sensitive method to investigate the critical current density J_c of high temperature superconducting thin films [1]. The ac field amplitude dependence of the ac susceptibility of structured narrow rings provides the experimental foundation for this method. Within the Bean model and via the determination of the so-called penetration field H_p (at which the perfect diamagnetic shielding is lost) and geometry parameters we obtain J_c . In this work we have exploited this technique at zero dc magnetic field H_{dc} to investigate the influence of the structuring method used to fabricate the high-temperature superconducting rings on J_c . Our results indicate clearly that ion beam etching is a far less destructive structuring technique than laser ablation.

We have also obtained the dc field dependence of J_c and analysed the effects of flux creep with an extended Bean model which enables the interpretation of the frequency dependence of the ac susceptibility associated with a finite resistivity due to flux motion [2]. We have analyzed the shift of the ac susceptibility with frequency and applied a scaling relation which has been predicted by Brandt [3]. Within this theory we have determined the flux creep exponent $n(T, H_{dc})$ and compared it with the one determined by relaxation measurements with a

SQUID.

The paper is organized as follows. In the next section we give a brief summary of the measured samples and experimental details. In section III we provide a theoretical resume of the ac response of narrow superconducting rings as well as the determination of the flux creep exponent from ac susceptibility. The results are described in section IV. A brief summary is given in section V.

II. EXPERIMENTAL DETAILS AND INVESTIGATED SAMPLES

The ac susceptibility measurements were performed with a Lake Shore 7000 AC Susceptometer designed for operation at low-level ac magnetic field amplitudes $H_0 \leq 2$ mT. We applied dc magnetic fields up to 3 T by a superconducting solenoid.

We have studied rings made from $\text{YBa}_2\text{Cu}_3\text{O}_{7-\delta}$ high-temperature superconducting 200 nm thin films prepared by pulsed laser deposition on 1 mm thick Al_2O_3 substrates with a critical temperature between $T_c = 89$ K and 90 K [4,5]. A 30 nm CeO_2 buffer layer was used. All the films were characterized by ac susceptibility measurements before structuring. Results on the films can be found in [6]. The films were structured by two methods: (a) by laser ablation (LA) with an excimer workstation having an optical resolution of $1.5\mu\text{m}$ and (b) by ion beam etching (IE). For the ion beam etching procedure a spun-on $1.5\mu\text{m}$ thick resist layer (AZ1450) was structured by excimer laser ablation using a scanning method. The resist was etched by laser apart from a thin, ~ 200 nm thick remaining film to prevent any damage of the superconducting layer. We used ion beam sputtering with argon to transfer the mask structure into the film. The ion etching was performed in a non-commercial IBE system with a base pressure better than 2×10^{-6} mbar equipped with a Kaufman type ion beam source operating at a beam energy of 700 eV and current density of 0.2 mA/cm^2 . The beam was neutralized by means of a hot filament to prevent charge accumulation on the sample surface. The samples were mounted on a water-cooled and rotating sample holder to avoid an excessive increase of temperature during etching. Table I shows the main characteristics of the measured samples.

III. THEORY

A. AC Susceptibility of Narrow Superconducting Rings

In this section we briefly review the ac response of narrow superconducting rings as described in [1,3]. We discuss the limit of a thin narrow ring of width w much smaller than the mean radius R , $R - w/2 \leq r \leq R + w/2$. Within the Bean model the virgin magnetization curve completely determines the hysteresis loop which has the shape of a parallelogram [7,8]. From these loops one obtains the complex susceptibility $\chi = \chi' - i\chi''$ of a superconducting narrow ring with constant J_c . For cycled magnetic field $H_a(t) = H_0 \sin \omega t$ we define the nonlinear susceptibility, the quantity we measure, as

$$\chi(H_0) = \frac{\omega}{V\pi H_0} \int_0^{2\pi} m(t) e^{-i\omega t} dt. \quad (1)$$

where m is the magnetic moment and V the sample volume. The virgin magnetization curve of such a ring is composed of two straight lines, $m(H_a) = (H_a/H_p)m_{sat}$ for $H_a \leq H_p$ and $m(H_a) = m_{sat}$ for $H_a \geq H_p$, since the screening supercurrent in the ring is limited to a maximum value $I_c = J_c d w$ (d is the ring thickness). As long as $|I| < I_c$ holds for the current induced in the ring by the applied field H_a , no magnetic flux can penetrate through the ring into the hole of the ring. When $|I| = I_c$ is reached the ring becomes transparent to magnetic flux. Therefore, when the applied field is increased further, flux lines will move through the ring as described in [9,10]. These authors treat the superconducting strip with transport current in an applied field. With the moving flux lines in the ring, magnetic flux enters the ring hole until the screening supercurrent decreases again to the value I_c . The magnetic moment $m = \pi R^2 I$ of the ring thus saturates at the value $m_{sat} = \pi R^2 I_c$. The applied field value H_p at which this saturation is reached follows from the inductivity L of the flat narrow ring [11], $L = \mu_0 R (\ln 8R/w - a)$ with $a \simeq 0.5$ [12].

The magnetic flux generated in the hole by a ring current I is $\Phi = LI$. As long as $I < I_c$ one has ideal screening, thus $\Phi = -\pi R^2 \mu_0 H_a$. Equating these two fluxes one obtains for the flat ring $I = \Phi/L = -\pi R H_a / [\ln 8R/w - a]$. At $H_a = H_p$ one reaches $|I| = I_c = J_c w d$, thus $H_p = [\ln 8R/w - a] I_c / \pi R$. Therefore, one can express J_c as

$$J_c = \frac{\pi R}{w d \left[\ln \frac{8R}{w} - \frac{1}{2} \right]} H_p. \quad (2)$$

The formulae given above are accurate to corrections of order $w/2R$ since the precise values of m and L depend on the current distribution across the ring width w which changes during the magnetization process.

With Eq. (1) and the expressions for $m(t)$ which are given in [3] we obtain the susceptibility of the ring normalized to the initial value $\chi(0) = -1$, i.e., to $\chi \rightarrow \chi V/m'(0)$,

$$\begin{aligned} \chi'(h) &= -1, & \chi''(h) &= 0, & h &\leq 1, \\ \chi'(h) &= -\frac{1}{2} - \frac{1}{\pi} \arcsin s + \frac{1}{\pi} s \sqrt{1-s^2}, \\ \chi''(h) &= \frac{4}{\pi} \frac{h-1}{h^2}, & h &\geq 1, \end{aligned} \quad (3)$$

with $h = H_0/H_P$ and $s = 2/h - 1$. These theoretical results have been confirmed experimentally in a previous paper [1]. We use expression (2) to determine J_c from the measured penetration field H_p .

B. Flux Creep Exponent from ac Susceptibility

For high enough dc magnetic fields, the influence of flux creep should be taken into account in the ac response of the superconducting ring. In our analysis we use a current voltage law $E = E(J)$ that is connected to a logarithmic dependence [13,14] of the pinning potential on the current density $U(J) = U_0 \ln(J_c/J)$ and describes flux creep as an activated motion of vortices which have to overcome this potential. Following [14] we have

$$E(J) = E_c \exp^{-\frac{U(J)}{kT}} = E_c \left(\frac{J}{J_c} \right)^n, \quad (4)$$

where $n(T, H) = U_0(T, H)/kT$ is the so-called flux creep exponent. The power law in Eq. (4) includes the limiting cases of Bean-like field distribution for which $n = \infty$ and of Ohmic dissipation for which $n = 1$.

By investigating the frequency (f) dependence of narrow rings under the application of a harmonic ac field $H_a(t) = H_0 \sin(\omega t)$ during flux creep, e.g. $1 < n < \infty$, Brandt [3] derived a scaling law for the frequency and magnetic field amplitude which states the following: The complex ac susceptibility at fixed temperature $\chi(T, f, H) = \chi' - i\chi''$ remains unchanged under the simultaneous transformation of time by a constant factor C , e.g. $t \rightarrow t/C$, and magnetic field by a factor C^β , e.g. $H \rightarrow HC^\beta$, with $\beta = 1/(n-1)$. This is equivalent to state that the following equation holds:

$$\chi(T, f, H) = \chi(T, fC, HC^\beta). \quad (5)$$

Using this property we determined the flux creep exponent $n(T, H)$ at different T and applied dc fields H_{dc} by measuring the ac susceptibility at different frequencies $f_0, f_1, f_2 \dots f_i$ and by equating the ac fields at which the same susceptibility is measured, i.e.

$$H_i = H_0 C^\beta = H_0 (f_i/f_0)^{\frac{1}{n-1}}, \quad (6)$$

where C is determined by the frequency ratio $C = f_i/f_0$. Equation (6) is a power law for the magnetic field amplitude. Plotting $\ln H$ vs. $\ln f$ should then give a straight

line of slope $\beta = 1/(n - 1)$.

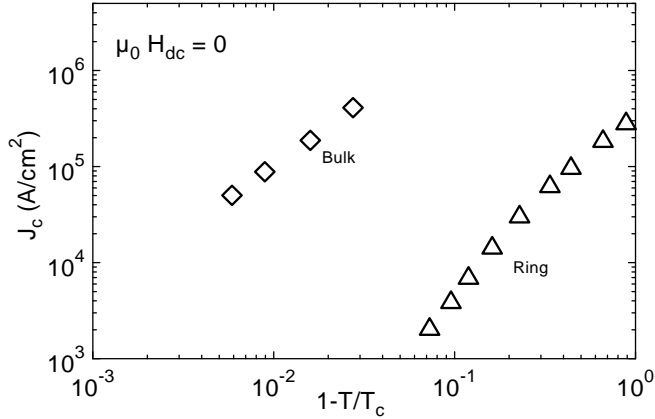


FIG. 1. Critical current density at zero applied dc field of sample LA2 as a function of reduced temperature. Note the strong decrease in J_c after structuring by laser ablation.

Jönsson-Åkerman et al. recently confirmed the scaling relation for the nonlinear ac susceptibility response of $\text{HgBa}_2\text{CaCu}_2\text{O}_{6+\delta}$ thin films [15]. In a previous work [16] the flux creep exponent n was determined from the frequency dependence of χ' in the limit of large ac amplitudes. In what follows we present a further confirmation of the scaling relation (5) by applying it on structured thin rings. Furthermore, we use a straightforward analysis procedure to obtain the field dependence of the pinning potential U_0 for fields up to 2T.

IV. RESULTS

A. Influence of the structuring method on J_c

In [1] a drastic decrease of J_c after structuring the films into rings was found. This behavior has been explained by the existence of microcracks in the path of the ring. In this paper we show that the structuring technology used to fabricate the superconducting ring has a large influence on its J_c .

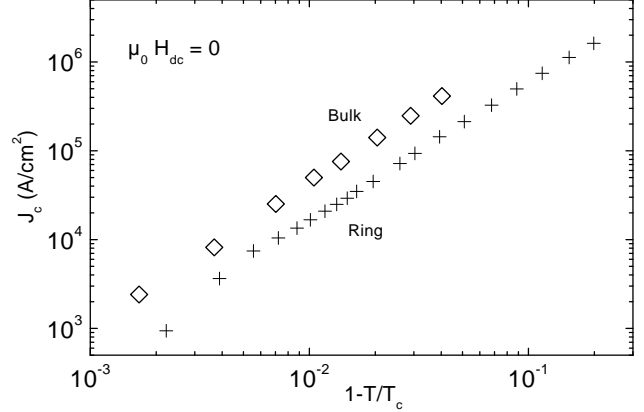


FIG. 2. Critical current density at zero applied dc field of sample IE1 as a function of reduced temperature. The patterning of the film by ion beam etching produces a relatively small decrease of J_c .

Figure 1 shows the temperature dependence of the critical current density J_c for sample LA2 before and after structuring by laser ablation. For this sample and before structuring J_c is 500 times larger than its value after structuring. For comparison the J_c values for the sample IE1 before and after structuring by ion beam etching are given in Fig. 2. For the ring of this sample J_c is reduced only 30 % compared to the unstructured sample. For all measured samples we have found that J_c of the measured LA-Rings is at least 100 times smaller than J_c before structuring. On the other hand the results for the IE-rings vary only a few percent.

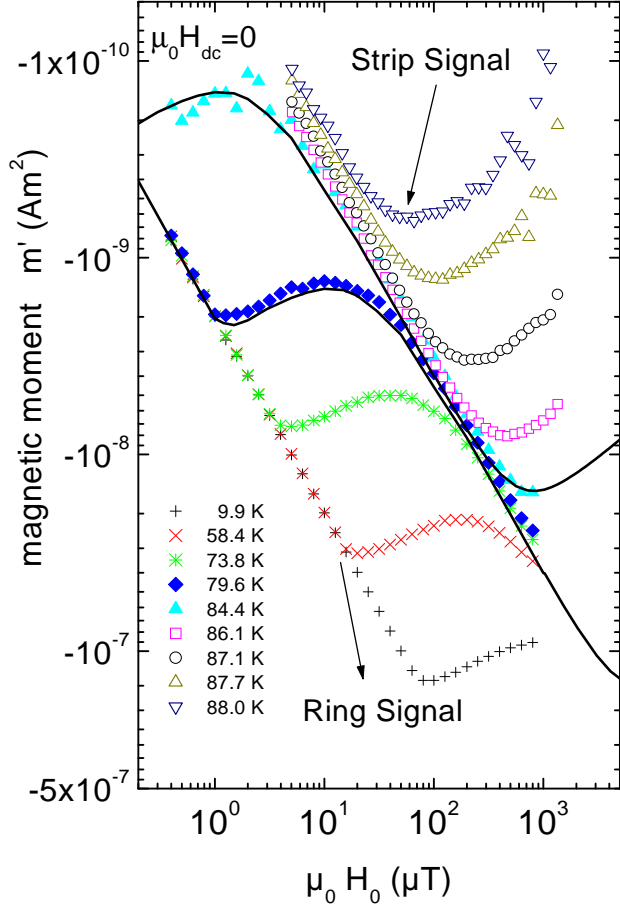


FIG. 3. In-phase component of the magnetic moment of sample LA2 as a function of applied ac field at different temperatures. The continuous lines were calculated using Eq. (3) assuming an overlap of the response of a ring with the corresponding strip signal [17] with a ratio $J_c^{\text{strip}} \approx 3000 J_c^{\text{ring}}$.

On the origin of the remarkable difference in J_c of the rings structured by laser ablation we speculate as follows. During treatment by the laser the tiny region within the laser spot is heated up to several thousands Kelvin for a few milliseconds. Because of the bad thermal conductivity of the substrate the temperature of the film rises to several hundred degrees in a small region around the spot as well.

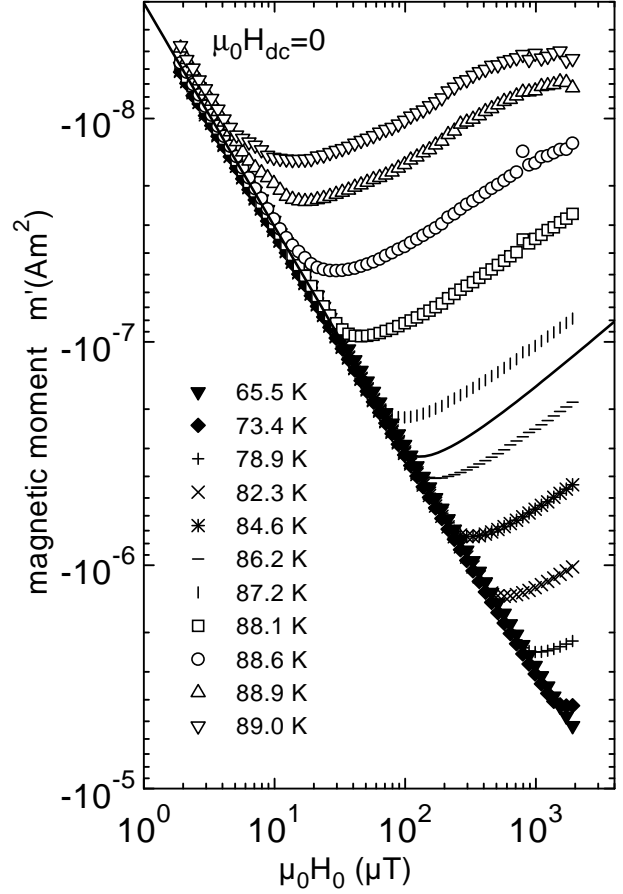


FIG. 4. In-phase component of the magnetic moment of sample IE1 as a function of applied ac field at different temperatures. The continuous line was calculated using Eq. (3).

It is known that heating can change the oxygen concentration of $\text{YBa}_2\text{Cu}_3\text{O}_{7-\delta}$. As a result the superconducting properties at the edges of the structured path may be altered up to the complete loss of superconductivity. Also, thermally induced shock waves may produce microcracks within the width of the ring and degrade the maximum critical current density. Our measurements of the thickness profile of the ring after structuring indicate a region of $\leq 5\mu\text{m}$ at the edges of the ring where the film appears to be completely damaged. In contrast we found sharp edges on films structured by ion beam etching.

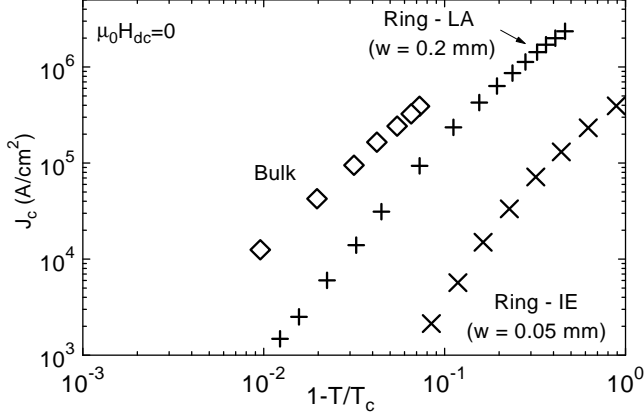


FIG. 5. Comparison of the critical current density as a function of reduced temperature for consecutive patterning sample LA1 by laser ablation (Ring-LA) and ion beam etching (Ring-IE).

To compare both structuring methods we can use a better way to present the data by plotting the in phase component of the magnetic moment $m' = \chi' H_a V$ as a function of the ac magnetic field amplitude. This is shown for the rings LA2, Fig. 3 and IE1, Fig. 4. The LA-ring in Fig. 3 shows a clear two-step-transition, one in the low-field-range and the other in the high-field range. We recognize a crossover from the ring with a lower J_c to the bulk signal for a long strip [17], see Fig. 3. On the other hand the IE-ring in Fig. 4 shows only a slight deviation from the expected ideal ring behavior (continuous line in Fig. 4) very probably due to small inhomogeneities within the ring.

To check whether the laser ablation structuring process leads to a “homogeneous” or “inhomogeneous” J_c over the width of the ring we structured sample LA1 once more by ion beam etching from a width of 0.2 mm to 0.05 mm. Whereas in the “homogeneous” case we do not expect a change in the measured J_c in the “inhomogeneous” case a different value for J_c should be measured due to the existence of islands with higher or lower critical current density. In Fig. 5 the results for the two consecutive structuring procedures are shown. We assign the observed decrease in J_c after the second structuring to tiny islands of lower J_c which are along the path of the ring with smaller width and were created after the first laser ablation structuring, indicating strongly inhomogeneous film properties.

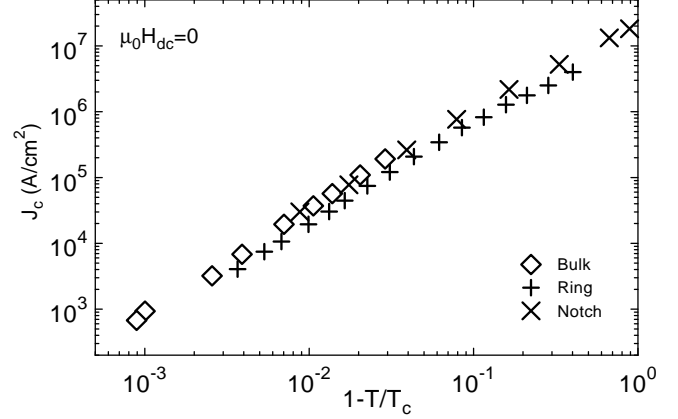


FIG. 6. Comparison of the critical current density as a function of reduced temperature of the ring prepared by ion beam etching in which we subsequently cut a notch (sample N).

In a similar experiment we reduced the width of the IE-ring (notch) by cutting a notch into it by ion beam etching, leaving only a small (16 μm) path where the current can flow. By this means we basically measure J_c in the path region. Figure 6 presents the critical current density corresponding to bulk, ring and ring-notch signal. Within experimental uncertainty J_c remains unchanged. This result supports the assumption of a homogeneous J_c in the film. Ion beam etching is therefore a far less destructive structuring technique than laser ablation.

B. Field Dependence of the Pinning Potential

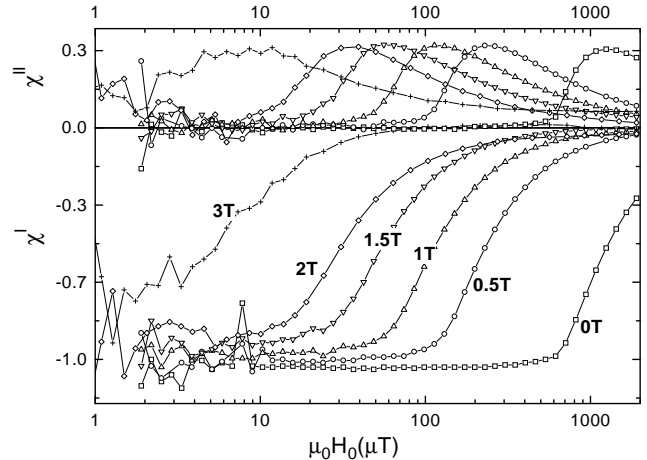


FIG. 7. Ac field amplitude dependence of the normalized ac susceptibility $\chi = \chi' - i\chi''$ for dc fields up to 3T at constant temperature $T = 79.8\text{K}$, Ring IE2.

For the measurements presented in this section we have chosen rings with highest critical current density

and with different radius to width ratios, e.g. rings IE1 and IE2. Together with a dc bias field the small ac perturbation $\mu_0 H_0 < 2\text{mT}$ was applied. In Fig. 7 one recognizes that the dc bias field mainly shifts χ_{max}'' to lower ac amplitudes and leaves the dependence of χ on the ac field amplitude essentially unaltered. This behavior is due to a decrease in the critical current density that determines the field $H_p \propto J_c$ at which the magnetic flux enters into the center of the ring.

During the increase of the applied dc field a current is induced in the ring. As described in section III A perfect shielding occurs as long as the current density is below the critical one. At currents larger than J_c flux can move into the center until the critical value is reached again. At large dc fields the magnetic moment of the ring thus saturates at a value that is determined by the shielding capability of the ring which is given by the critical current related to the specific dc field. By applying then a harmonic ac signal to the ring, its magnetic moment has a hysteresis loop around the static dc bias field similar as for $H_{dc} = 0$.

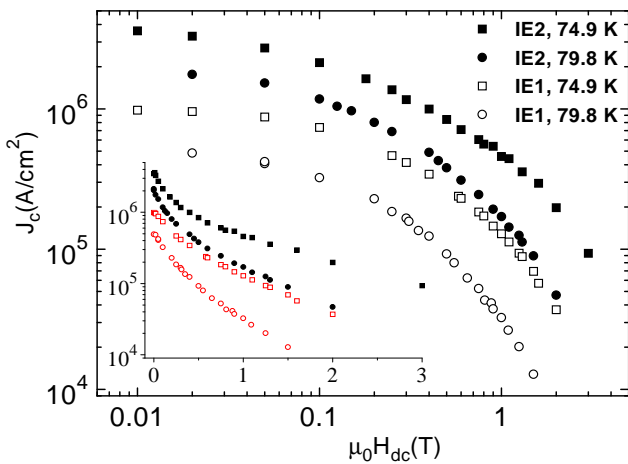


FIG. 8. Dc field dependence of the critical current density at two different temperatures in a log-log plot, derived from the shift of the penetration field H_p for the rings IE1 and IE2. The inset shows the same data plotted in a semi-log plot.

Since the application of the dc field leads to flux penetration it will influence the pinning of vortices in the ring material as well. By this means the flux creep exponent $n = U_0/kT$ is altered. In Fig. 7 an increase in flux creep can be found for large dc fields. As predicted by Brandt [3] a slight smoothing of χ'' or χ' around the penetration field H_p is observed for increasing dc field, i.e. decreasing n . From the shift of H_p with dc field one can determine the field dependence of J_c shown in Fig. 8. The field dependence of J_c we obtain is similar to that measured by vibrating reed experiments in Y123 thin films [18]. The observed field dependence of J_c can be understood within the collective pinning theory for

three dimensional pinning mechanism [19]. Three dimensional pinning is assumed since the correlation length of the vortex lines along the field direction is smaller than the thickness of the films [18]. The magnetic field independence of J_c observed at low fields indicate that the vortices are pinned independently, i.e. the single vortex pinning regime. At higher fields the interaction between flux lines leads to the formation of flux bundles which are pinned collectively and therefore J_c decreases with field.

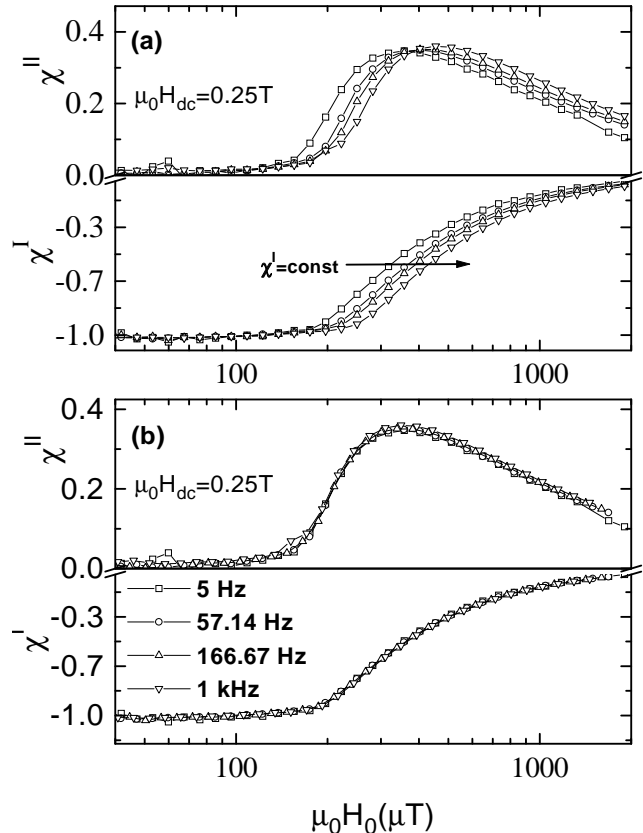


FIG. 9. (a) Ac field amplitude dependence of the normalized ac susceptibility for frequencies 5; 57.14; 166.67; 1000 Hz for the ring IE2, at $T=79.8\text{K}$ and $\mu_0 H_{dc} = 0.25\text{T}$. The value χ' at which the frequency shift is analyzed is indicated by the horizontal arrow in the plot. The corresponding ac field amplitudes are $\mu_0 H_0 = 300; 338.9; 358.1; 395.8 \mu\text{T}$. (b) Re-scaled plots using Eq. (6) with $n = 20.2$ derived as outlined in section III B.

In what follows we concentrate on the field dependence of the pinning potential U_0 . For a series of dc fields we measured the amplitude dependence of χ' at four different frequencies. Such a scan can be seen in Fig. 9(a) for the ring IE2. In a step by step procedure we determine the ac field amplitudes corresponding to the frequencies for a fixed value of χ' where the slope is largest. This

is indicated by the arrow in Fig. 9(a). Then we plot the logarithm of the obtained magnetic ac field amplitudes versus the logarithm of the respective frequencies, see Fig. 10, and by performing a linear fit we determine the corresponding slope $\beta = 1/(n - 1)$ for different dc fields. Within the available frequency range this plot gives straight lines for fixed dc field and temperature as theoretically [3] expected. This gives the flux creep exponent n for fixed temperature and dc field, see Eq. (6). Figure 9(b) shows the rescaling of all four curves in (a) following Eqs. (4) and (5) and using the obtained value for n . In routine measurements one only needs to measure χ around the maximum in χ'' to determine the shift of χ' with frequency (only 15 to 20 points per scan). The necessary information on the ac field amplitude range to be measured at each dc field can be obtained by a preliminary scan. Within 20 hours we were thus able to measure the scans required to determine $n(T, H_{dc})$ for 10 dc fields at one fixed temperature.

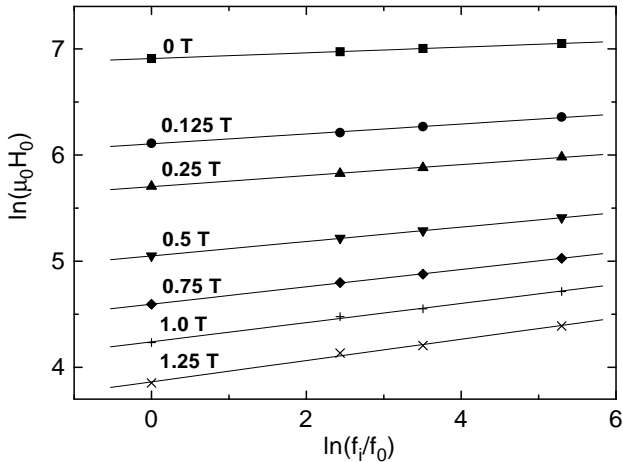


FIG. 10. Frequency shift of the ac field amplitude in a log-log scale for the ring IE2 at $T=79.8\text{K}$. The frequencies are $f_0 = 5\text{Hz}$, $f_i = 57.14; 166.67; 1000\text{Hz}$. From the slope of the obtained linear fit the flux creep exponent n is determined, see section III B for details. For 0.25T the corresponding ac amplitude scans are shown in Fig. (9).

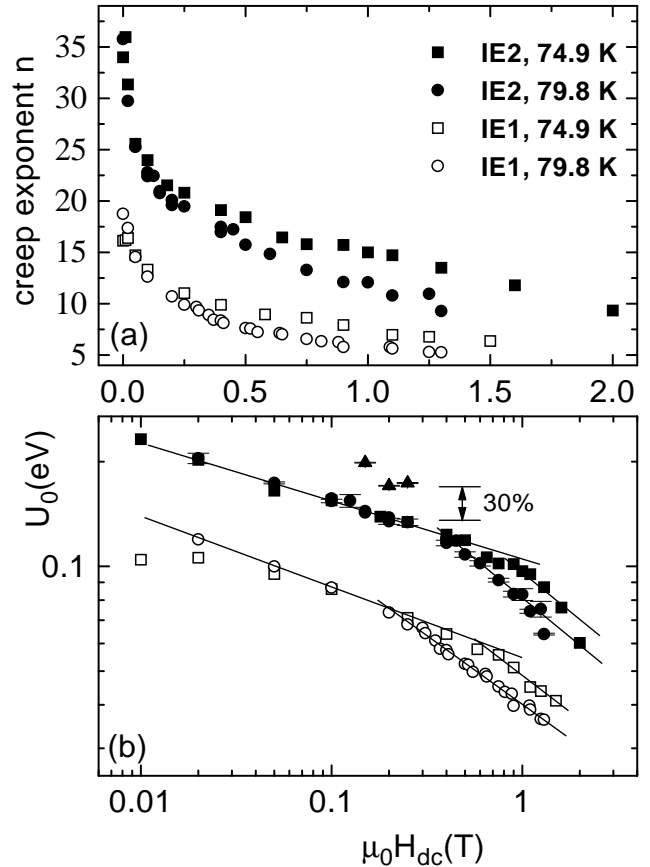


FIG. 11. Dc field dependence of (a) the flux creep exponent n and (b) the pinning potential U_0 for the rings IE1 and IE2 at $T=74.9\text{K}$ and 79.8K . Values are derived from the scaling relation outlined in section III B. Large n at zero dc field correspond to a Bean-like behavior for the ac response of structured thin rings. (b) Power law fits (continuous lines) $U_0 \propto H_{dc}^{-\alpha}$ give $\alpha \approx 0.2$ and $0.4-0.7$ for the low- and high-field regions respectively. For comparison the values $U_0(H_{dc})$ obtained from relaxation measurements, see Fig. 12, are plotted with solid up-triangles.

Scans for the two selected rings and temperatures $T=74.9\text{K}$ and $T=79.8\text{K}$ have been performed and analyzed in this manner. The dependence of the flux creep exponent $n(T, H_{dc})$ and the pinning potential $U_0(T, H_{dc})$ on dc field are shown in Fig. 11. In Fig. 11(a) one clearly sees the strong decrease of n with dc field. It can be also noted that n increases the lower the temperature of the ring. The large values of $n \approx 20 - 40$ at $H_{dc} = 0$ for both rings are consistent with the little frequency dependence of the ac response at low dc fields. For this reason the Bean model is a good approximation in this limit. At the same T and H_{dc} we find $n_{IE2} > n_{IE1}$. We assign this difference in n between the two rings to variations in

the film properties from which the rings were structured.

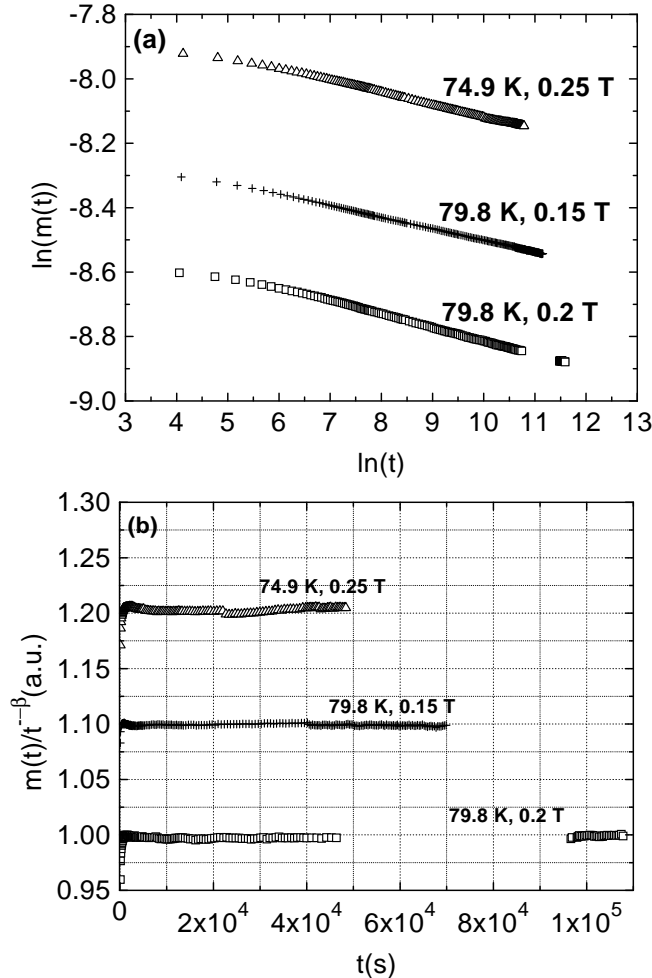


FIG. 12. (a) Log-log plot of the relaxation of the magnetic moment $m(t)$ for the ring IE2, after the external dc field has been decreased to the constant value $\mu_0 H_{dc}$ as indicated in the figure. From the slope we obtain $n = 26.9$ (74.9 K, 0.25 T), 28.9 (79.8 K, 0.15 T), 24.8 (79.8 K, 0.20 T), see Eq. (7). (b) Time independence of $m(t)/t^{-\beta}$ calculated with the respective exponents $\beta = 1/(n - 1)$ obtained from (a). The curves were normalized for convenience.

The same qualitative statement holds for J_c as well, see Fig. 8. In Fig. 11(b) one notes for both rings a similar dependence of U_0 on H_{dc} . We distinguish a low- and a high-field region in which we obtain straight lines in a double logarithmic plot. Assuming a power law for the field dependence of U_0 , e.g. $U_0 \propto H_{dc}^{-\alpha}$, we obtain exponents $\alpha \approx 0.2$ and $\alpha \approx 0.4 - 0.7$ in the low- and high-field regions, respectively. At $T = 100$ K and in a dc field range between 20 and 100 Oe a similar dc field dependence for the flux creep exponent $n \propto H_{dc}^{-0.18}$ has

been recently observed for $\text{HgBa}_2\text{CaCu}_2\text{O}_{6+\delta}$ thin films ($T_c = 120$ K) [15].

Figure 11(b) also shows the values for U_0 obtained from relaxation measurements. We used this technique to verify our results by an independent method. In the presence of flux creep the magnetic moment $m(t)$ relaxes after ramping of the external field H_{dc} to some value. After a transient time τ one observes the universal relaxation [20,3]

$$m(t) \propto (t/\tau)^{-\beta}. \quad (7)$$

With a SQUID magnetometer we have performed three relaxation measurements with the ring IE2. The results are shown in Fig. 12(a). Following Eq. (7) we obtain the flux creep exponent n and hence the pinning potential U_0 from a linear fit in the double logarithmic plot. With the respective values for $n = (1 + \beta)/\beta$, $m(t)/t^{-\beta}$ vs. t should be time independent. This is nicely confirmed in Fig. 12(b). A similar time dependence with $n \simeq 20$ at $H_{dc} = 1$ T has been obtained for the irreversible magnetization of $\text{Bi}_2\text{Sr}_2\text{Ca}_2\text{Cu}_3\text{O}_{10}$ samples below 20 K [21]. As shown in Fig. 11(b), the relaxation measurements provide values for the pinning potential U_0 which are similar to those obtained with the nonlinear ac susceptibility scaling procedure.

V. CONCLUSIONS

In this work we have used the nonlinear ac susceptibility method on structured $\text{YBa}_2\text{Cu}_3\text{O}_{7-\delta}$ high-temperature superconducting rings to study the influence of different patterning methods to the critical current density of the films. The nonlinear susceptibility method applied on superconducting rings of small enough widths is a suitable method to identify regions with degraded superconducting properties. We have found that laser ablation structuring degrades the superconducting properties of the film, decreasing strongly its critical current density and introducing inhomogeneities within $\sim 100\mu\text{m}$ from the patterned edges. In contrast, the ion beam etching procedure is a far less destructive technique. Measuring the nonlinear susceptibility of the rings at different frequencies we reconfirmed the recently proposed scaling relation for the frequency and field amplitude dependence. The scaling relation allows us to obtain the field dependence of the flux creep exponent or pinning potential at different temperatures. Our results show a power law dependence for the flux creep exponent $n \propto H_{dc}^{-0.2}$ for fields below ~ 0.2 T and at reduced temperatures $0.8 < T/T_c < 0.9$.

ACKNOWLEDGMENTS

The authors thank M. Lorenz for providing us with the thin films. This work was supported by the German-

Israeli Foundation for Scientific Research and Development (Grant G-0553-191.14/97) and by the Innovationsskolleg "Phänomene an den Miniaturisierungsgrenzen" (DFG IK 24/B1-1).

- [1] F. Mrowka, M. Wurlitzer, P. Esquinazi, E. H. Brandt, M. Lorenz and K. Zimmer, *Appl. Phys. Lett.* **70**, 898 (1997).
- [2] For a review see, e.g., E. H. Brandt, *Rep. Prog. Phys.* **58**, 1465 (1995).
- [3] E. H. Brandt, *Phys. Rev. B* **55**, 14513 (1997).
- [4] M. Lorenz, H. Hochmuth, D. Natusch, H. Börner and K. Kreher, *MRS Proceedings*, Vol. 341 (MRS, Pittsburgh, 1994), p. 189.
- [5] M. Lorenz, H. Hochmuth, D. Natusch, H. Börner, G. Lippold, K. Kreher and W. Schmitz, *Appl. Phys. Lett.* **68**, 3332 (1996).
- [6] M. Wurlitzer, M. Lorenz, K. Zimmer and P. Esquinazi, *Phys. Rev. B* **55**, 11816 (1997).
- [7] T. Ishida and H. Mazaki, *J. Appl. Phys.* **52**, 6798 (1981).
- [8] J. Gilchrist and M. Konczykowski, *Physica C* **212**, 43 (1993).
- [9] E. H. Brandt and M. V. Indenbom and A. Forkl, *Europhys. Lett.* **22**, 735 (1993).
- [10] E. H. Brandt and M. Indenbom, *Phys. Rev. B* **48**, 12893 (1993).
- [11] J. Gilchrist and E. H. Brandt, *Phys. Rev. B* **54**, 3530 (1996).
- [12] L. D. Landau and E. M. Lifshitz, *Electrodynamics of Continuous Media*, Vol. III of theoretical Physics (Pergamon, Oxford, 1963).
- [13] E. Zeldov, N. M. Amer, G. Koren, A. Gupta, M. W. McElfresh, and R. J. Gambino, *Appl. Phys. Lett.* **56**, 680 (1990).
- [14] V. M. Vinokur, M. V. Feigel'man and V. B. Geshkenbein, *Phys. Rev. Lett.* **67**, 915 (1991).
- [15] B. J. Jönsson-Åkerman, R. V. Rao and E. H. Brandt, *Phys. Rev. B* **60**, 14913 (1999).
- [16] B. J. Jönsson, K. V. Rao, S. H. Yun and U. O. Karlsson, *Phys. Rev. B* **58**, 5862 (1998).
- [17] E. H. Brandt, *Phys. Rev. B* **49**, 9024 (1994); **50**, 4034 (1994).
- [18] M. Ziese and P. Esquinazi, *Z. Phys. B* **94**, 265 (1994).
- [19] M. U. Feigel'man, V. M. Vinokur, *Phys. Rev. B* **41**, 8986 (1990).
- [20] E. H. Brandt, *Phys. Rev. Lett.* **76**, 4030 (1996).
- [21] V. V. Makarov, Y. Kopelevich and S. Moehlecke, *Physica C* **264**, 213 (1996).

TABLE I. Characteristics of the measured rings. The structuring methods were laser ablation (LA) and ion beam etching (IE). R denotes the radius of the ring, w its width, T_c and J_c (77 K) the critical temperature and critical current density at zero applied field. J_c was calculated using Eq. (2).

sample	structuring method	R (mm)	w (mm)	before structuring		after structuring	
				T_c (K)	J_c (77 K)	T_c (K)	J_c (77 K)
LA1	LA	1	0.2	≈ 89	$4.5 \times 10^6 \text{ A/cm}^2$	≈ 89	$3.5 \times 10^5 \text{ A/cm}^2$
	IE	1	0.05			≈ 89	$1.0 \times 10^4 \text{ A/cm}^2$
LA2	LA	1	0.1	≈ 89	$3.3 \times 10^6 \text{ A/cm}^2$	≈ 89	$7.9 \times 10^3 \text{ A/cm}^2$
IE1	IE	0.9	0.18	89.7	$3.3 \times 10^6 \text{ A/cm}^2$	89.8	$1.0 \times 10^6 \text{ A/cm}^2$
IE2	IE	0.9	0.1	89.8	$3.0 \times 10^6 \text{ A/cm}^2$	89.9	$1.8 \times 10^6 \text{ A/cm}^2$
N	IE	0.95	0.075	≈ 90	$2.8 \times 10^6 \text{ A/cm}^2$	89.9	$1.1 \times 10^6 \text{ A/cm}^2$
	notch	0.95	0.016			89.9	$1.9 \times 10^6 \text{ A/cm}^2$